

ORIGINAL ARTICLES

Comparison between mandibular malignant tumors and inflammatory lesions using ^{67}Ga scintigraphy: Relationship with panoramic radiography, CT and MRI findings

Ichiro Ogura^{*1}, Mikiko Sue¹, Takaaki Oda¹, Yoshihiko Sasaki¹, Kazuhide Hayama²

¹Radiology, The Nippon Dental University Niigata Hospital, Niigata, Japan

²Department of Oral and Maxillofacial Radiology, School of Life Dentistry at Niigata, The Nippon Dental University, Niigata, Japan

Received: May 10, 2017

Accepted: July 4, 2017

Online Published: July 9, 2017

DOI: 10.5430/ijdi.v4n2p67

URL: <https://doi.org/10.5430/ijdi.v4n2p67>

ABSTRACT

Purpose: Gallium ^{67}Ga scintigraphy is useful for the estimation of head and neck squamous cell carcinoma, especially tumor recurrence and distant metastases. We compared mandibular malignant tumors with inflammatory lesions using ^{67}Ga scintigraphy with multimodal imaging, such as panoramic radiography, CT and MRI.

Methods: Nineteen patients with mandibular malignant tumors (7 squamous cell carcinoma and 2 malignant lymphoma) and inflammatory lesions (6 osteoradionecrosis, 3 medication-related osteonecrosis of the jaw [MRONJ] and 1 osteomyelitis) underwent ^{67}Ga scintigraphy with panoramic radiography, CT and MRI. The statistical analysis with respect to comparison between imaging features of ^{67}Ga scintigraphy and lesions was performed with the Pearson's chi-squared test.

Results: ^{67}Ga scintigraphy for 2 of 2 patients with malignant lymphoma were positive (100%), 4 of 7 patients with squamous cell carcinoma were positive (57.1%), and 10 of 10 patients with inflammatory lesions were positive (100%) in the mandible. The detection of squamous cell carcinoma with ^{67}Ga scintigraphy was lower than that of inflammatory lesions ($p = .047$).

Conclusions: ^{67}Ga scintigraphy is useful for detection of malignant lymphoma and inflammatory lesions in the mandible.

Key Words: Gallium radioisotopes, Gamma cameras, Carcinoma, Inflammation, Mandible

1. INTRODUCTION

Gallium ^{67}Ga scintigraphy is an effective technique for the differentiation of oral malignant tumors from benign tumors or inflammatory disease.^[1] ^{67}Ga scintigraphy is useful for the estimation of head and neck squamous cell carcinoma, especially tumor recurrence and distant metastases.^[2,3] However, in recent years, PET using the radiolabeled glucose

analogue 18F-fluorodeoxyglucose has shown its potential to detect distant metastases.^[4-7]

Excepting for squamous cell carcinoma, some authors have reported that ^{67}Ga scintigraphy is useful in the differentiation of malignant lymphoma,^[8] sarcoidosis^[9-11] and other inflammatory diseases.^[12,13] However, to the best of our knowledge, ^{67}Ga scintigraphy with panoramic radiography,

*Correspondence: Ichiro Ogura; Email: ogura@ngt.ndu.ac.jp; Address: Radiology, The Nippon Dental University Niigata Hospital, 1-8 Hamaura-cho, Chuo-ku, Niigata, Niigata 951-8580, Japan.

CT and MRI in comparison between mandibular malignant tumors and inflammatory diseases have not been reported in the literature. We compared mandibular malignant tumors with inflammatory lesions using ^{67}Ga scintigraphy with panoramic radiography, CT and MRI.

2. MATERIALS AND METHODS

2.1 Patient population

The ethics committee of our institution approved this retrospective study. After providing written informed consent, 19 patients (11 men, 8 women; range age 53-95 years, mean age 70.7 years) with malignant tumors (7 squamous cell carcinoma and 2 malignant lymphoma) and inflammatory lesions (6 osteoradionecrosis, 3 medication-related osteonecrosis of the jaw [MRONJ] and 1 osteomyelitis) in the mandible underwent ^{67}Ga scintigraphy with panoramic radiography, CT and MRI at our university hospital from October 2013 to February 2017. The histopathological diagnoses were obtained by surgery or biopsy in all cases.

2.2 Image acquisition

Panoramic radiographs was performed with a panoramic machine (Veraviewepocs; J MORITA MFG, Kyoto, Japan) using the maxillofacial protocol at our hospital: tube voltage, 70 kV; tube current, 10 mA.

CT imaging was performed with a 16-multidetector CT scanner (Aquilion TSX-101A; Toshiba Medical Systems, Otawara, Japan) using the maxillofacial protocol at our hospital: tube voltage, 120 kV; tube current, 150 mAs; field of view, 240×240 mm; rotation time, 0.5 sec; axial acquisition, 0.50 mm. The patients received contrast enhanced CT (CECT) with nonionic iodine for head and neck lesions. One nonionic contrast media was used: Iohexol 300 mgI/ml (Omnipaque 300 Syringe, Daiichi-Sankyo, Tokyo, Japan). Contrast medium was administered as an injection of 100 ml at a rate of 2.0 ml/s (Autoenhance A-250, Nemoto-Kyorindo, Tokyo, Japan).

The MR images (1.5 Tesla MR unit; EXCELART Vantage MRT-2003; Toshiba Medical Systems, Otawara, Japan) with a head coil included unenhanced axial T1-weighted imaging (T1WI; repetition time (TR) 660 ms, echo time (TE) 12 ms), T2-weighted imaging (T2WI; TR 4,000 ms, TE 120 ms), short TI inversion recovery images (STIR; TR 2,500 ms, TE 15 ms, TI 190 ms). After an injection of contrast medium (gadobutrol; Gadovist 1.0mol/L Syringe, Bayer, Osaka, Japan; 0.1 mL/kg), axial and coronal T1WI were acquired.

^{67}Ga scintigraphy was performed with a SNC-5100R (Shimadzu, Kyoto, Japan) and a Scintipack 24,000 (Shimadzu) with a 512×512 matrix at 72 hours after the injection, im-

ages were recorded on the computer at 6 min/frame. The radiopharmaceutical used in this study was ^{67}Ga -citrate (Gallium Citrate- ^{67}Ga Injection, FUJIFILM RI Pharma, Tokyo, Japan). Each patient was administered the agent at 185 MBq with a rapid intravenous injection. The stored data were displayed on a screen for analysis.

2.3 Image analysis

For patients with mandibular malignant tumors and inflammatory lesions, imaging features of ^{67}Ga scintigraphy, panoramic radiography, CT and MRI were independently analyzed by 2 oral and maxillofacial radiologists. ^{67}Ga scintigraphy were classified into 2 groups:^[1] positive, where the intensity of ^{67}Ga in the lesion area was higher than that in the surrounding normal area, and negative, where the intensity of ^{67}Ga in the lesion area was the same as in the surrounding normal area. Any discrepancies of the imaging evaluation were resolved by consensus of the 2 oral and maxillofacial radiologists.

2.4 Statistical analysis

The statistical analysis with respect to comparison between imaging features of ^{67}Ga scintigraphy and lesions was performed with the Pearson's chi-squared test using the statistical package IBM SPSS Statistics, version 24 (IBM Japan, Tokyo, Japan). A P value lower than 0.05 was considered as statistically significant.

3. RESULTS

Table 1 shows imaging features of malignant tumors and inflammatory diseases in the mandible with ^{67}Ga scintigraphy, panoramic radiography, CT and MRI.

Regarding malignant lymphoma (see Figure 1), panoramic radiography showed osteolytic changes in the jaws. Axial bone tissue algorithm CT revealed an osteolytic lesion with the destruction in the mandible. ^{67}Ga scintigraphy showed increased uptake. On MRI, axial T1WI showed homogeneous, low-signal intensity. T2-weighted image (T2WI) revealed heterogeneous, high-signal intensity. Post-contrast T1WI showed heterogeneous enhancement.

Regarding squamous cell carcinoma (see Figure 2), panoramic radiography revealed a moth-eaten appearance in the jaws. Axial bone tissue algorithm CT showed an osteolytic lesion with the destruction in the mandible. ^{67}Ga scintigraphy showed increased uptake in the mandible and submandibular region. On MRI, axial T1WI showed homogeneous, low-signal intensity. Post-contrast T1WI showed heterogeneous enhancement. Axial contrast-enhanced CT image showed submandibular lymph node with rim-enhancement.

Table 1. Imaging features of malignant tumors and inflammatory diseases in the mandible with ⁶⁷Ga scintigraphy, panoramic radiography, CT and MRI

Case	Age (years)	Gender	Lesion	⁶⁷ Ga scintigraphy	Panoramic radiography	CT findings	MRI findings
1	54	female	lymphoma	positive	did not undergo examination	did not undergo examination	heterogeneous enhancement
2	71	male	lymphoma	positive	osteolytic changes	osteolytic lesion with the destruction	heterogeneous enhancement
3	61	male	SCC	positive	moth-eaten appearance	osteolytic lesion with the destruction	heterogeneous enhancement
4	63	male	SCC	positive	moth-eaten appearance	osteolytic lesion with the destruction	heterogeneous enhancement
5	75	female	SCC	negative	no evidence of disease	no evidence of disease	no evidence of disease
6	76	male	SCC	negative	no evidence of disease	did not evaluate because of metal artifact	heterogeneous enhancement
7	79	female	SCC	negative	extracted tooth fossa, sclerotic lesions	osteolytic change, sclerotic lesions	heterogeneous enhancement
8	83	female	SCC	positive	moth-eaten appearance	osteolytic lesion with the destruction	heterogeneous enhancement
9	95	male	SCC	positive	moth-eaten appearance	osteolytic lesion with the destruction	heterogeneous enhancement
10	65	female	MRONJ	positive	osteolytic change, sclerotic lesions	osteolytic change, sclerotic lesions, sequestrum, periosteal bone proliferation	heterogeneous, high-signal intensity on T2WI and STIR
11	70	female	MRONJ	positive	osteolytic change, sclerotic lesions	osteolytic change, sclerotic lesions, sequestrum	heterogeneous, high-signal intensity on T2WI and STIR
12	84	female	MRONJ	positive	osteolytic change, sclerotic lesions	osteolytic change, sclerotic lesions, sequestrum	heterogeneous, high-signal intensity on T2WI and STIR
13	53	male	ORN	positive	osteolytic change, sclerotic lesions	osteolytic change, sclerotic lesions, sequestrum, periosteal bone proliferation	heterogeneous, high-signal intensity on T2WI and STIR
14	64	male	ORN	positive	osteolytic change, sclerotic lesions	osteolytic change, sclerotic lesions, sequestrum	heterogeneous, high-signal intensity on T2WI and STIR
15	65	male	ORN	positive	osteolytic change, sclerotic lesions	osteolytic change, sclerotic lesions, sequestrum	heterogeneous, high-signal intensity on T2WI and STIR
16	67	male	ORN	positive	osteolytic change, sclerotic lesions	osteolytic change, sclerotic lesions, sequestrum	heterogeneous, high-signal intensity on T2WI and STIR
17	69	male	ORN	positive	osteolytic change, sclerotic lesions	osteolytic change, sclerotic lesions, sequestrum, periosteal bone proliferation	heterogeneous, high-signal intensity on T2WI and STIR
18	72	female	ORN	positive	osteolytic change, sclerotic lesions	osteolytic change, sclerotic lesions, sequestrum	heterogeneous, high-signal intensity on T2WI and STIR
19	78	male	osteomyelitis	positive	osteolytic change, sclerotic lesions	osteolytic change, sclerotic lesions	heterogeneous, high-signal intensity on T2WI and STIR

Note. SCC: squamous cell carcinoma; MRONJ: medication-related osteonecrosis of the jaw; ORN: osteoradionecrosis, T2WI: T2-weighted image; STIR: short TI inversion recovery image.

Regarding MRONJ (see Figure 3), panoramic radiography showed osteolytic changes in the jaws and sclerotic lesions. Axial bone tissue algorithm CT revealed an osteolytic changes in the jaws, sclerotic lesions, sequestrum separation, and periosteal bone proliferation. ⁶⁷Ga scintigraphy showed

increased uptake. On MRI, axial T1WI showed homogeneous, low-signal intensity in the mandible and spread of soft tissue inflammation to buccal space. T2WI and STIR showed heterogeneous, high-signal intensity in the mandible and spread of soft tissue inflammation to buccal space.

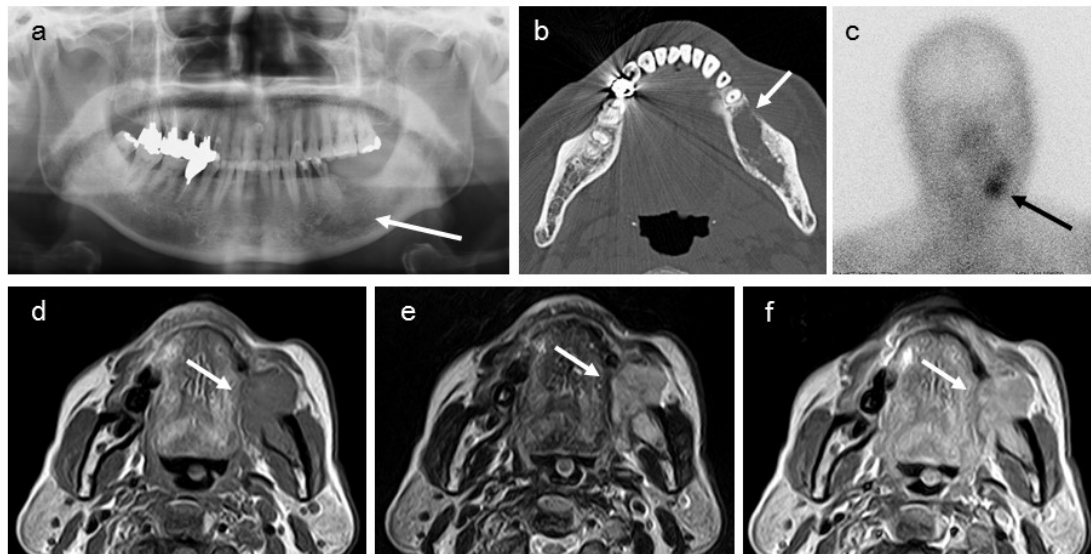


Figure 1. Malignant lymphoma of the left side of the mandible in a 71-year-old male

a. Panoramic radiography shows osteolytic changes in the jaws (arrow); b. Axial bone tissue algorithm CT shows an osteolytic lesion with the destruction of buccal cortex in the left mandible (arrow); c. ⁶⁷Ga scintigraphy shows increased uptake (arrow); d. On MRI, axial T1-weighted image (T1WI) revealed homogeneous, low-signal intensity (arrow); e. T2-weighted image (T2WI) revealed heterogeneous, high-signal intensity (arrow); f. Post-contrast T1WI showed heterogeneous enhancement (arrow)

Regarding osteoradionecrosis (see Figure 4), panoramic radiography showed osteolytic changes in the jaws and sclerotic lesions. Axial bone tissue algorithm CT revealed an osteolytic changes in the jaws, sclerotic lesions and sequestrum separation. ⁶⁷Ga scintigraphy showed increased uptake. On

MRI, axial T1WI showed homogeneous, low-signal intensity in the mandible and spread of soft tissue inflammation to buccal space. T2WI and STIR showed heterogeneous, high-signal intensity in the mandible and spread of soft tissue inflammation to buccal space.

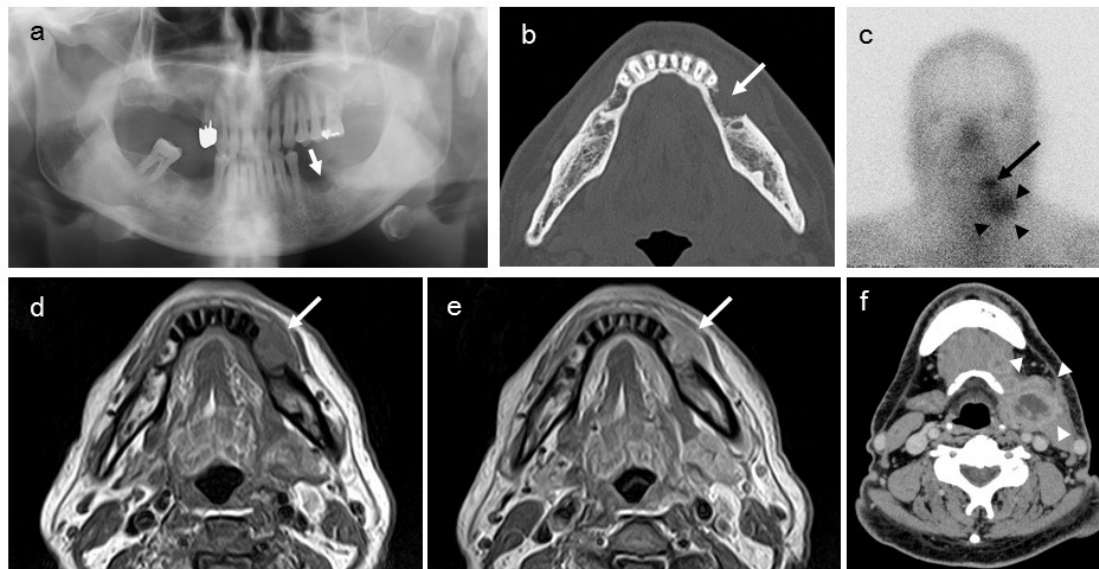


Figure 2. Squamous cell carcinoma of the left side of the mandible in a 63-year-old male

a. Panoramic radiography shows a moth-eaten appearance in the jaws (arrow); b. Axial bone tissue algorithm CT shows an osteolytic lesion with the destruction of buccal cortex in the left mandible (arrow); c. ⁶⁷Ga scintigraphy shows increased uptake in the mandible (arrow) and submandibular region (arrowheads); d. On MRI, axial T1WI revealed homogeneous, low-signal intensity (arrow); e. Post-contrast T1WI showed heterogeneous enhancement (arrow); f. Axial contrast-enhanced CT image shows submandibular lymph node with rim-enhancement (arrowheads)

Table 2 shows the comparison between imaging features of ⁶⁷Ga scintigraphy and lesions. The ⁶⁷Ga scintigraphy for 2 of 2 patients with malignant lymphoma were positive (100%); 4 of 7 patients with squamous cell carcinoma were

positive (57.1%), and 10 of 10 patients with inflammatory lesions were positive (100%) in the mandible. The detection of squamous cell carcinoma with ⁶⁷Ga scintigraphy was lower than that of inflammatory lesions ($p = .047$).

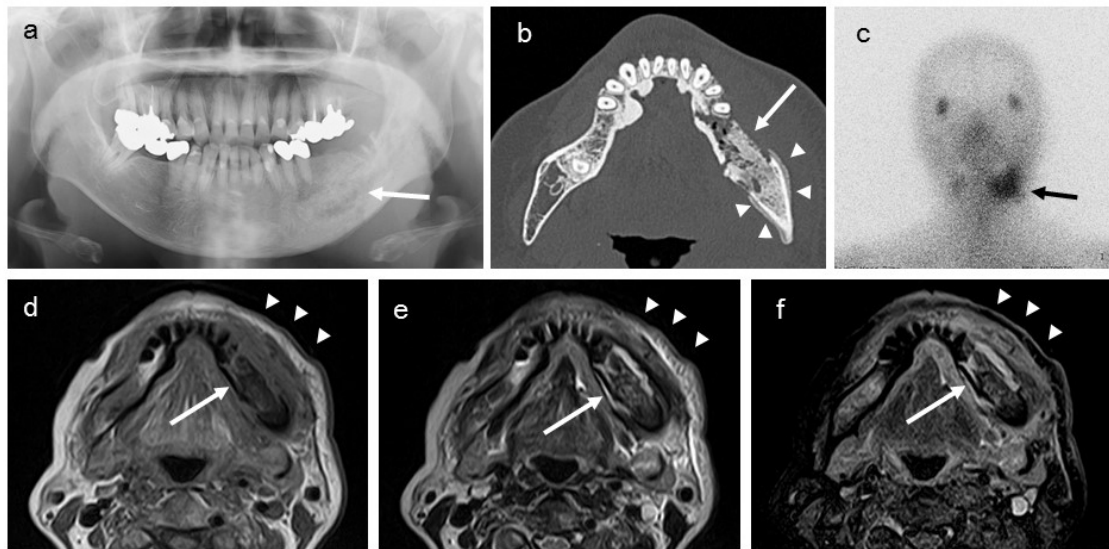


Figure 3. MRONJ of the left side of the mandible in a 65-year-old female

a. Panoramic radiography shows osteolytic changes in the jaws and sclerotic lesions (arrow); b. Axial bone tissue algorithm CT shows an osteolytic changes in the jaws, sclerotic lesions, sequestrum separation (arrow), and periosteal bone proliferation (arrowheads); c. ⁶⁷Ga scintigraphy shows increased uptake (arrow); d. On MRI, axial T1WI revealed homogeneous, low-signal intensity in the mandible (arrow) and spread of soft tissue inflammation to buccal space (arrowheads); e, f. T2WI and short TI inversion recovery (STIR) revealed heterogeneous, high-signal intensity in the mandible (arrow) and spread of soft tissue inflammation to buccal space (arrowheads)

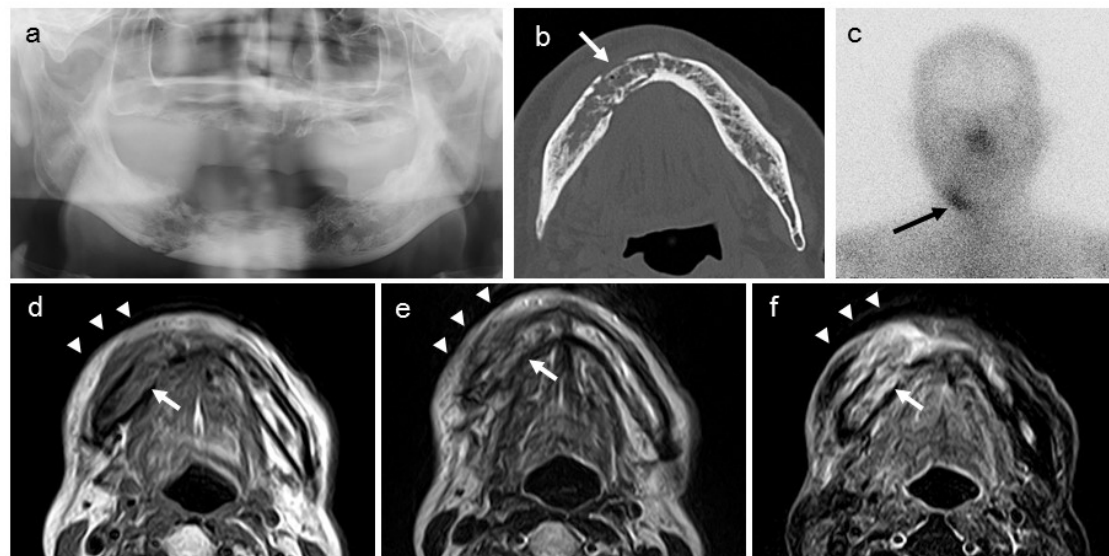


Figure 4. Osteoradionecrosis of the right side of the mandible in a 65-year-old male

a. Panoramic radiography shows osteolytic changes in the jaws and sclerotic lesions (arrow); b. Axial bone tissue algorithm CT shows an osteolytic changes in the jaws, sclerotic lesions and sequestrum separation (arrow); c. ⁶⁷Ga scintigraphy shows increased uptake (arrow); d. On MRI, axial T1WI revealed homogeneous, low-signal intensity in the mandible (arrow) and spread of soft tissue inflammation to buccal space (arrowheads); e, f. T2WI and STIR revealed heterogeneous, high-signal intensity in the mandible (arrow) and spread of soft tissue inflammation to buccal space (arrowheads)

Table 2. ⁶⁷Ga scanning results of malignant tumor and inflammatory diseases

Lesions	Number of cases	Result of ⁶⁷ Ga scanning	
		Positive	Negative
Malignant tumor	9	6 (66.7%)	3 (33.3%)
Malignant lymphoma	2	2 (100%)	0 (0%)
Squamous cell carcinoma	7	4 (57.1%)	3 (42.9%)
Inflammatory diseases	10	10 (100%)	0 (0%)

Note. *p* = .047

4. DISCUSSION

The ⁶⁷Ga scintigraphy has been widely used to detect squamous cell carcinoma^[1,3] and malignant lymphoma^[8] of the head and neck. In our study, the ⁶⁷Ga scintigraphy for 2 of 2 patients with malignant lymphoma were positive (100%), and 4 of 7 patients with squamous cell carcinoma were positive (57.1%).

Regarding mechanism of ⁶⁷Ga accumulation in tumors, Tsan et al.^[14] showed that ⁶⁷Ga was delivered to the tumor through capillaries with increased permeability, and ⁶⁷Ga binding proteins might also contribute to the accumulation and retention of ⁶⁷Ga in tumors. We showed that images for 3 out of 7 patients who had squamous cell carcinoma were negative (42.9%) in the ⁶⁷Ga scintigraphy. These 3 cases (case 5-7) were small size of tumors. We consider that the size of tumors also is a factor of the degree of ⁶⁷Ga accumulation in lesions, furthermore, relationship between negative ⁶⁷Ga scintigraphy for SCC and T staging of the tumor.

Regarding malignant lymphoma, in our study, the ⁶⁷Ga scintigraphy for 2 of 2 patients with malignant lymphoma were positive (100%). However, Okada et al.^[8] showed that PET is replacing ⁶⁷Ga scintigraphy in the diagnosis and management of malignant lymphoma.

In this study, the ⁶⁷Ga scintigraphy for 10 of 10 patients with inflammatory diseases were positive (100%). Li et al.^[1] indicated that ⁶⁷Ga scintigraphy for 2 of 11 patients who had chronic inflammatory diseases (1/4 parotitis, 1/5 submaxillaritis and 0/2 lymphadenitis) were positive (18.2%).

Tsan et al.^[14] showed that some in tumors may be taken up by inflammatory cells when they are present. Furthermore, Keijsers et al.^[9] showed imaging the inflammatory activity of sarcoidosis, namely, overall sensitivity to detect active sarcoidosis was 88% for ⁶⁷Ga scintigraphy. Ishii et al.^[10] showed that ⁶⁷Ga scintigraphy was useful in differentiating between sarcoidosis and IgG4-related disease. Tsai et al.^[13] suggested that the kidney uptake index from the absolute quantitative renal ⁶⁷Ga scintigraphy may be a useful parameter for evaluating the disease activity in lupus nephritis. Consequently, the authors consider that ⁶⁷Ga scintigraphy was more useful for inflammatory lesions than malignant tumors, and a combination of ^{99m}Tc MDP and ⁶⁷Ga scintigraphy can used to help diagnose osteomyelitis as indications of scintigraphy. Furthermore, we recommend the ⁶⁷Ga scintigraphy with panoramic radiography, CT and MRI for detection of malignant tumors and inflammatory diseases.

There were several limitations of this study. The sample was relatively small. Moreover, several types of tumors and inflammatory lesions in the mandible. Therefore, further research is necessary to validate these results.

5. CONCLUSIONS

We compared mandibular malignant tumors with inflammatory lesions using ⁶⁷Ga scintigraphy with panoramic radiography, CT and MRI. ⁶⁷Ga scintigraphy is useful for detection of malignant lymphoma and inflammatory lesions in the mandible.

ACKNOWLEDGEMENTS

The authors wish to thank Professor Y. Okada, Department of Pathology, The Nippon Dental University School of Life Dentistry at Niigata and Professor M. Tsuchimochi, Department of Oral and Maxillofacial Radiology. This work was supported by NDU Grants N-16020.

CONFLICTS OF INTEREST DISCLOSURE

The authors reported no conflicts of interest related to this study.

REFERENCES

[1] Li N, Zhu W, Zuo S, et al. Value of gallium-67 scanning in differentiation of malignant tumors from benign tumors or inflammatory disease in the oral and maxillofacial region. *Oral Surg Oral Med Oral Pathol Oral Radiol Endod.* 2003; 96: 361-7. [https://doi.org/10.1016/S1079-2104\(03\)00349-4](https://doi.org/10.1016/S1079-2104(03)00349-4)

[2] Murata Y, Ishida R, Umehara I, et al. ⁶⁷Ga whole-body scintigraphy in the evaluation of head and neck squamous cell carcinoma. *Nucl Med Commun.* 1999; 20: 599-607. PMID:10423761 <https://doi.org/10.1097/00006231-199907000-00002>

[3] Kosuda S, Kadota Y, Umeda S, et al. Does supplementation of CT and MRI with gallium-67 SPECT improve the differentiation between benign and malignant tumors of the head and neck? *Ann Nucl Med.* 2003; 17: 475-80. PMID:14575383 <https://doi.org/10.1007/BF03006438>

[4] Kitagawa Y, Nishizawa S, Sano K, et al. Prospective comparison of 18F-FDG PET with conventional imaging modalities (MRI, CT, and ⁶⁷Ga scintigraphy) in assessment of combined intraarterial chemotherapy and radiotherapy for head and neck carcinoma. *J Nucl Med.* 2003; 44: 198-206. PMID:12571209

- [5] Corey AS, Hudgins PA. Radiographic imaging of human papillomavirus related carcinomas of the oropharynx. *Head Neck Pathol.* 2012; 6: S25-40. PMID:22782221 <https://doi.org/10.1007/s12105-012-0374-3>
- [6] Plaxton NA, Brandon DC, Corey AS, et al. Characteristics and limitations of FDG PET/CT for imaging of squamous cell carcinoma of the head and neck: a comprehensive review of anatomy, metastatic pathways, and image findings. *AJR Am J Roentgenol.* 2015; 205: W519-31. PMID:26496574 <https://doi.org/10.2214/AJR.14.12828>
- [7] Senft A, Hoekstra OS, Witte BI, et al. Screening for distant metastases in head and neck cancer patients using FDG-PET and chest CT: validation of an algorithm. *Eur Arch Otorhinolaryngol.* 2016; 273: 2643-50. PMID:26350882 <https://doi.org/10.1007/s00405-015-3773-8>
- [8] Okada M, Sato N, Ishii K, et al. FDG PET/CT versus CT, MR imaging, and 67 Ga scintigraphy in the posttherapy evaluation of malignant lymphoma. *Radiographics.* 2010; 30: 939-57. PMID:20631361 <https://doi.org/10.1148/rg.304095150>
- [9] Keijsers RG, Grutters JC, Thomeer M, et al. Imaging the inflammatory activity of sarcoidosis: sensitivity and inter observer agreement of 67Ga imaging and 18F-FDG PET. *Q J Nucl Med Mol Imaging.* 2011; 55: 66-71. PMID:21242947
- [10] Ishii S, Miyajima M, Sakuma K, et al. Comparison between sarcoidosis and IgG4-related disease by whole-body 67Ga scintigraphy. *Nucl Med Commun.* 2013; 34: 13-8. PMID:23044518 <https://doi.org/10.1097/MNM.0b013e32835a2eea>
- [11] Shim H, Joo J, Choi HJ, et al. Lack of increased FDG uptake in the lacrimal and salivary glands in patients with sarcoidosis and potential underlying mechanism. *Clin Nucl Med.* 2016; 41: 274-7. PMID:26825201 <https://doi.org/10.1097/RLU.0000000000001127>
- [12] Aslangul E, M'bemba J, Caillat-Vigneron N, et al. Diagnosing diabetic foot osteomyelitis in patients without signs of soft tissue infection by coupling hybrid 67Ga SPECT/CT with bedside percutaneous bone puncture. *Diabetes Care.* 2013; 36: 2203-10. PMID:23514729 <https://doi.org/10.2337/dc12-2108>
- [13] Tsai SC, Hsieh TY, Huang PW, et al. Absolute quantitative evaluation of 67Ga scintigraphy in lupus nephritis. *Clin Nucl Med.* 2016; 41: 442-6. PMID:26825210 <https://doi.org/10.1097/RLU.0000000000001108>
- [14] Tsan MF, Scheffel U. Mechanism of gallium-67 accumulation in tumors. *J Nucl Med.* 1986; 27: 1215-9. PMID:3522824